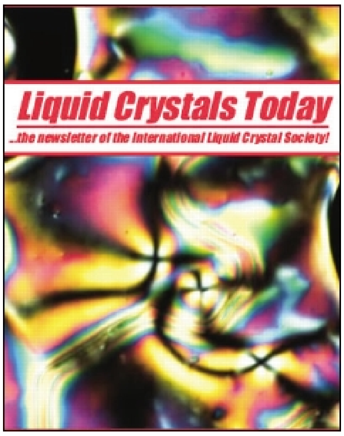

Liquid Crystals Today
Publication details, including instructions for authors and subscription information:
http://www.informaworld.com/smpp/title~content=t713681230

In-plane switching electro-optical effect of nematic liquid crystals

Masahito Oh-e

Online publication date: 11 November 2010

To cite this Article Oh-e, Masahito(2001) 'In-plane switching electro-optical effect of nematic liquid crystals', Liquid Crystals Today, 10: 2, 6 — 10
To link to this Article: DOI: 10.1080/14645180110074800
URL: http://dx.doi.org/10.1080/14645180110074800

In-plane switching electro-optical effect of nematic liquid crystals

MASAHITO OH-E
Hitachi Ltd., Displays, 3300 Hayano, Mobara-shi, Chiba-ken, 297-8622 Japan;
e-mail: ooe-masahito@mobara.hitachi.co.jp

This report describes the physical principles underlying the switching of nematic liquid crystals (LCs) by an electric field in the plane of the substrate. The results have contributed to development of an IPS-mode-TFT-LCD, which is now commercially available and one of the most popular TFT-LCDs with ultra-wide viewing angle characteristics. The report summarizes work in the Glenn Brown prize winning PhD thesis, Tokyo Institute of Technology, 2-12-1 O-okayama, Meguro-ku, Tokyo, 152-8551 Japan.

1. Introduction

In recent years, Liquid Crystal Display (LCD) technology has made great progress in terms of display quality. However, further advances in LCD technology required improvement of the narrow and limited viewing angle characteristics that had been an inherent drawback of the conventional twisted nematic (TN) electro-optical effect [1]. Therefore, how the viewing angle characteristics could be overcome was studied in detail [2]. An in-plane switching (IPS) electro-optical effect of a nematic liquid crystal was combined with a thin film transistor (TFT) driving scheme to successfully provide an advanced LCD having ultra-wide viewing angle characteristics [3–5]. Figure 1 reproduces images from oblique viewing directions which demonstrate the IPS and conventional TN effects. It is clear that the IPS effect is a very attractive display mode, providing an excellent viewing angle characteristic.

In this article, the IPS effect is discussed to get ideas on how LC materials can be optimized for devices using this technology. Firstly, the electro-optical and switching principles of a nematic LC governed by an in-plane electric field are described. Secondly, we show how the IPS effect differs from the TN effect in terms of the voltage-holding ratio (VHR) characteristic, which provides a way of choosing a variety of LC materials. Finally, the LC materials applicable to the IPS effect are discussed.

2. Electro-optical principles

Figure 2 shows schematically how the IPS effect displays field-off (dark) and field-on (bright) states [1–6]. Basically, no electric field is needed for the dark state, because the optical axis in the LC layer is in the same direction as the polarization axis of the polarizer, with the arrangement of the polarizer and analyser being at right angles. This configuration plays an important role in blocking the light and generates a purely dark state. While the electric field is gradually applied to the LC layer, rotation of the optical axis in the substrate plane

Figure 1. Display images of the IPS TFT-LCD and the TN TFT-LCD viewed from different directions.

Liquid Crystals Today ISSN 1464-5181 online © 2001 Taylor & Francis Ltd
http://www.tandf.co.uk/journals
DOI: 10.1080/14645180110074800

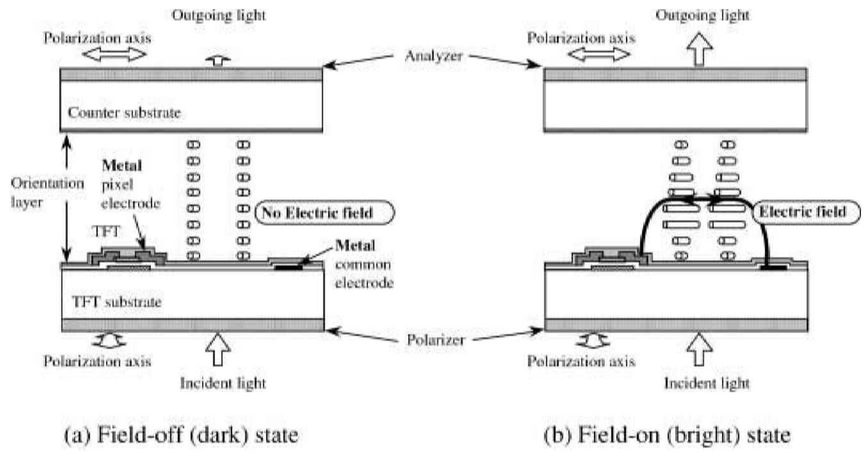

Figure 2. The IPS electro-optical effect showing (*a*) field-off (dark) and (*b*) field-on (bright) states.

allows the incident light to be transmitted, because phase retardation is generated in the LC layer. When the angle between the averaged director of the LC and the polarization axis is just 45°, the maximum bright state is realized. The condition to get the brightest outgoing beam is that the retardation of the LC layer is equivalent to half a wavelength.

One of the reasons why the IPS effect has better viewing angle characteristics is closely related to how the dark state is generated [7]. The transmittance of light passing through the uniaxial medium is given by [8]

$$\frac{T}{T_0} = \sin^2(2\chi)\cdot\sin^2\left(\frac{\pi d\cdot\Delta n(\theta,\phi)}{\lambda}\right), \tag{1}$$

where χ is the angle between the direction of polarization of the incident light and the optical axis of the uniaxial medium, $\Delta n(\theta, \phi)$ symbolizes the birefringence of the uniaxial medium which is dependent on the incident (θ) and azimuthal (ϕ) angles of the viewing direction with respect to the substrate normal direction, and λ is the wavelength of the light. The switching from a dark to a bright state is accomplished by changing the angle between the polarization direction of the incident light and the optical axis of the LC layer, which corresponds to the first sine term of equation (1). Another reason for the good viewing angle characteristics of the IPS effect is based on the in-plane motion of LC directors by the field. Due to the rod-like shape of LC molecules, the in-plane motion of the LC directors means there is relatively little dependence of viewing directions on birefringence, compared with the out-of plane motion of LC directors.

3. Switching mechanisms

Consideration is next given to how the LC switching is governed by the in-plane electric field [2, 6]. An in-plane electric field, applied to homogeneously aligned LC molecules, is assumed to be not only perpendicular to the LC directors, but also parallel to the substrate plane. The Fréedericksz transition can be analysed by the conventional procedure [9, 10]. Then, we have

$$V_c^{IPS} = E_c^{IPS} \times l = \frac{\pi l}{d}\sqrt{\frac{K_{IPS}}{\varepsilon_0\,|\Delta\varepsilon|}}, \tag{2}$$

where E_c^{IPS} is the threshold electric field for the LC being driven, l is the electrode distance from edge to edge, d is the cell gap, K_{IPS} is the elastic constant which is from a combination of splay, twist and bend deformations in actual switching, ε_0 is the vacuum dielectric constant and $\Delta\varepsilon$ is the dielectric anisotropy. This equation means that not only l determines V_c^{IPS}, but also d directly influences V_c^{IPS} at the same time. It is well known that an analogous relation V_c^{TN} is obtained for the case of the TN effect, differing only in the elastic constant term [1, 9, 11]. Applying the electric field perpendicular to the substrate plane yields the threshold voltage as $V_c^{TN} = E_c^{TN}\cdot d$ due to the equivalence of l and d. This means that the LC molecules in the electric field perpendicular to the substrate plane are driven by the voltage. However, this is not the case with LC molecules in an in-plane electric field parallel to the substrate plane. The electric field is independent of the LC layer normal direction and LC molecules are not governed by the voltage, but by the electric field itself in the IPS effect. Equation (2) predicts that the threshold voltage in the IPS effect is sensitive to the variation of d [12]. This is experimentally proven in figure 3 which shows that the threshold voltage is proportional to the reciprocal of the cell gap. As far as the dependence of the dielectric anisotropy of LCs on the switching behaviour is concerned, applying the LC that has negative dielectric anisotropy yields uniform switching between the electrodes [13].

The theory of dynamical response of the LC shows that the switching on and off times of the LC in the IPS

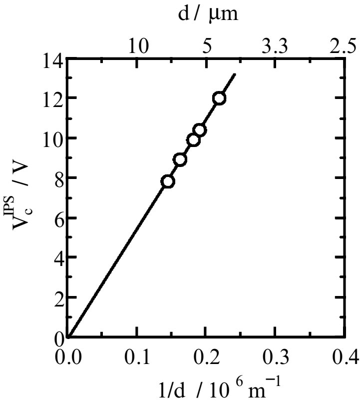

Figure 3. Cell gap effect on the threshold voltage. LC, ZLI-2806; interdigital electrode width, 10 µm; electrode distance, 15 µm.

effect are described by equation (3) [14];

$$\tau_{off} = \frac{\gamma_1 d^2}{\pi^2 K_{IPS}} = \frac{\gamma_1}{\varepsilon_0 |\Delta\varepsilon| (E_c^{IPS})^2}. \quad (3)$$

$$\tau_{on} = \frac{\gamma_1}{\varepsilon_0 |\Delta\varepsilon| E^2 - \frac{\pi^2}{d^2} K_{IPS}} = \frac{\gamma_1}{\varepsilon_0 |\Delta\varepsilon| (E^2 - E_c^2)},$$

Here, γ_1 is the twist-viscous coefficient.

Experimental data plotted in figure 4 show how the on and off times are affected by the electric field strength and the cell gap. These results agree with the predictions of equation (3). On the other hand, equation (3) indicates that γ_1 and K_{IPS} are significant for determining response time. If it is assumed that the same degree of twist deformation occurs in a layer, a larger elastic energy should exist in a thinner LC layer than in a thicker one. Another important point is that a faster response time cannot be expected by reduction of electrode distance, because LC molecules do respond to the electric field strength.

4. Voltage-holding ratio (VHR) characteristic

The VHR characteristic also differs for the IPS and the TN effects [15]. A low resistivity LC generally decreases VHR, but a higher VHR can be expected in the IPS effect than in the TN effect as shown in figure 5 (*a*). This makes it possible to combine a low resistivity LC with the TFT driving scheme in the IPS effect. This advantage is attributed to whether the electric field direction is parallel or perpendicular to the substrate plane. Figures 5 (*b*-1) and (*b*-2) present the equivalent circuit models that describe the IPS and TN cell structures, respectively. In the IPS effect, the LC layer is connected in parallel to an insulating layer, an orientation layer and even a substrate, when an equivalent electric circuit is applied. This parallel connection of the LC layer with other components can provide supplementary capacities for the relaxation of charges over the LC layer which are supplied by externally applied voltages during selected periods. As a result, the supplementary capacities can support the maintenance of the supplied voltages over the LC layer during nonselected periods. This finding should open new possibilities for the development of LC and orientation layer materials for TFT driving applications.

5. Optimization concept of LC materials

Knowing the above-mentioned electro-optical and electrical principles of the IPS effect, we can discuss how to suitably optimize the LC materials for this effect [2]. Among the required display characteristics of LCDs, the threshold voltage and response time are important ones to be considered. The IPS effect provides at least four additional parameters affecting the threshold voltage, i.e., thickness of the LC layer (the cell gap), the distance between neighbouring electrodes, the width of each electrode, and the rubbing direction. The threshold voltage is affected by the electrode width when the width is on the same order as the cell gap, or smaller, because the electric field distribution is varied by the change of

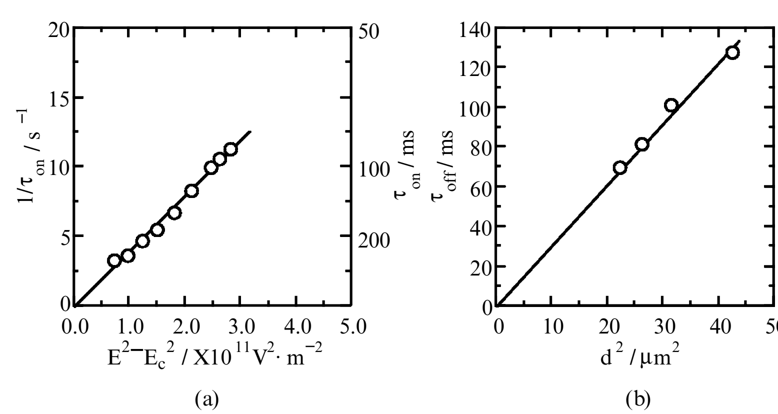

Figure 4. (*a*) τ_{on} vs. $E^2 - E_c^2$. (*b*) τ_{off} vs. d^2. LC, ZLI-2806. The interdigital electrode width is 10 µm; electrode distance is 15 µm.

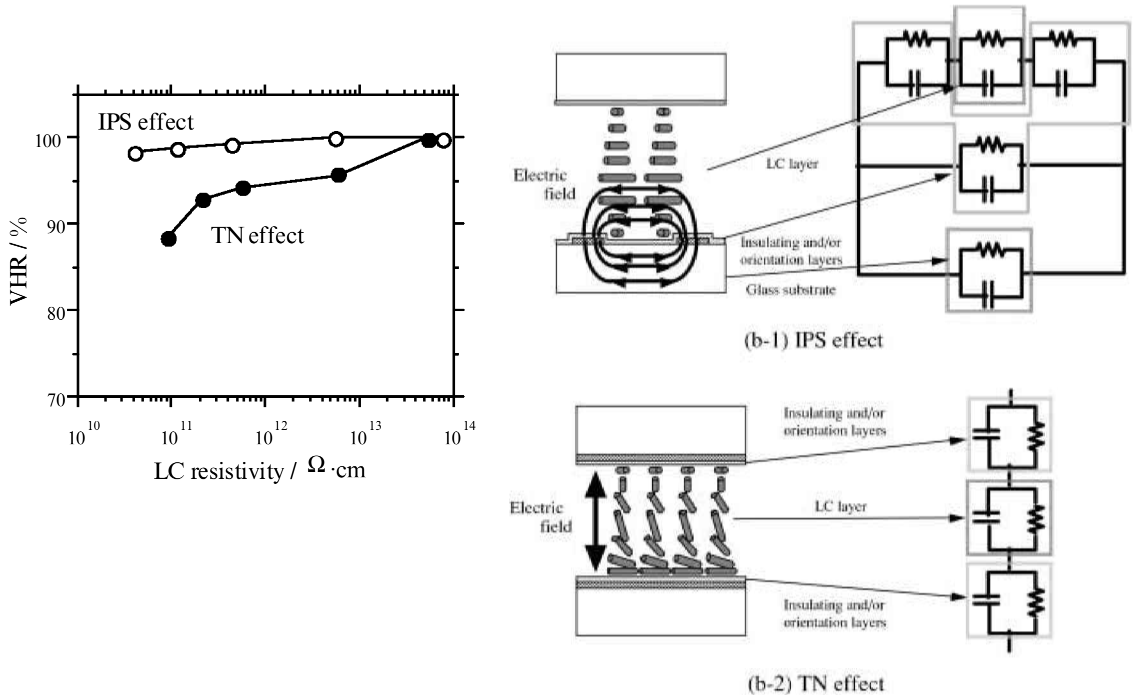

Figure 5. (*a*) VHR characteristics as a function of LC resistivity. (*b*) Equivalent circuit models for (*b*-1) the IPS effect and (*b*-2) the TN effect.

the electrode width. Thicker cell gap and narrower electrode distance are preferable to obtain lower threshold voltage, however, a thicker cell gap results in slower response speed and a narrower electrode distance is not relevant to the dynamical response time. So the optimization of performance in the IPS effect is more complicated than that in the TN effect. In this report we deal with the cell gap and the electrode distance. First, to avoid the influence of the variation of the cell gap on the threshold voltage, we introduce a driving voltage parameter (DVP or DVP'), i.e., the threshold voltage multiplied by the cell gap, or, in addition, divided by the electrode distance and given as [15]

$$DVP = V_c^{IPS} \times d = \pi l \sqrt{\frac{K_{IPS}}{\varepsilon_0 |\Delta\varepsilon|}},$$

or

$$DVP' = V_c^{IPS} \times \frac{d}{l} = \pi \sqrt{\frac{K_{IPS}}{\varepsilon_0 |\Delta\varepsilon|}}. \qquad (4)$$

for a response parameter (RP), we also find

$$RP = \frac{T_{\mathrm{off}}}{d^2} \propto \frac{\gamma_1}{\pi^2 K_{IPS}}. \qquad (5)$$

This equation evaluates the intrinsic response capacity of the LC materials without the electric field strength and the variation of the cell gap. It is possible to evaluate the LC materials for the driving voltage and the response time precisely, since these parameters include only the physical properties of LCs. Figure 6 shows an experimentally determined plot of the evaluation parameters for some LC mixtures consisting of terminally fluorinated LC substances, i.e., 3,4-difluoro-benzene and 3,4,5-trifluoro-

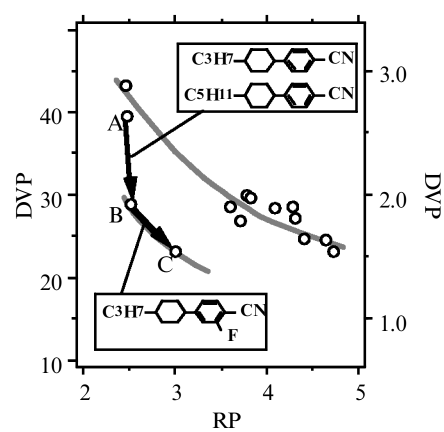

Figure 6. Plot of evaluation parameters for some LC materials and the results of the effect of doping cyano-substances into the LC mixtures. A is MLC-6252, B is a mixture, MLC-6252 doped with 15% 1-(4-cyanophenyl)-4-propylcyclohexane and 15% 1-(4-cyanophenyl)-4-pentylcyclohexane, and C is the further addition of 10% 4-cyano-1-(4-ethylbenzoyloxy)-3-fluorobenzene to mixture B. Other points represent mixtures composed of 3,4-difluoro-benzene and 3,4,5-trifluoro-benzene derivatives.

benzene derivatives, which were developed for the conventional TFT driving scheme. The difficulty is in satisfying a trade-off relationship between the driving voltage and response parameters, DVP' and RP, as long as the ratio of the twist viscous coefficient, γ_1, to the dielectric anisotropy, $\Delta\varepsilon$, does not change drastically. We then find the trade-off relationship:

$$DVP' = \sqrt{\frac{\gamma_1}{\varepsilon_0 |\Delta\varepsilon|} \times \frac{1}{RP}}. \qquad (6)$$

This relation tells us that a small twist viscous coefficient, γ_1, with large dielectric anisotropy, $\Delta\varepsilon$, can be effective to overcome the trade-off relationship between DVP' and RP so that DVP' decreases while keeping a certain smaller RP. In figure 6, we demonstrate how effective cyano-substances are for getting a breakthrough in the trade-off relationship so that it is possible to be in the parameter region that corresponds to a lower driving voltage while maintaining the faster response time. The lower resistivity caused by doping with cyano-substances gives an advantage in the VHR characteristic in the IPS effect. We also find another advantage in lower resistivity LCs that give rise to ionic flow so that the externally applied DC field can be reduced [2].

6. Summary

Optical characteristics: In the IPS effect, the viewing angle characteristics are far superior to those of the conventional twisted nematic effect.

Switching mechanism: A threshold field is proportional to the reciprocal of the cell gap. It is the electric field and not the voltage that drives the LCs. Consequently, the threshold voltage in the IPS effect is strongly dependent on the cell gap. The relaxation time of LCs is proportional to the square of the cell gap. A thinner cell gap results in a faster response time. The switching on time for an in-plane electric field is inversely proportional to the difference between the square of the field strength and the square of threshold field.

Electric characteristics: The voltage-holding ratio in the IPS effect is better than that in the conventional twisted nematic effect, even for LCs with much lower resistivity.

Optimization concept of LC materials for IPS eVect: Parameters have been established to optimize the driving voltage and response time. These parameters are effective for evaluating the physical properties of LCs. Cyano-substituted LCs prove to be effective to reduce driving voltage and response time.

This work was supported by Hitachi, Ltd. I gratefully acknowledge Professor Hideo Takezoe, Tokyo Institute of Technology (Japan), and Professor David A. Dunmur, University of Southampton (UK), for nominating this PhD thesis for the Glenn H. Brown Award given by ILCS. I also thank Professor Youkoh Kaizu, Tokyo Institute of Technology, and Dr Katsumi Kondo, Hitachi Research Laboratory for their suggestions and cordial advice during the preparation of the PhD thesis.

References

[1] Schadt, M., and Helfrich, W., 1971, *Appl. Phys. Lett.*, **18,** 127.
[2] See for example: Oh-e, M., and Kondo, K., 1997, *Liq. Cryst.*, **22,** 379 and references therein.
[3] Oh-e, M., Ohta, M., Aratani, S., and Kondo, K., 1995, *Proc. 15th Int. Display Res. Conf.* (SID, Hamamatsu), p. 577.
[4] Ohta, M., Oh-e, M., and Kondo, K., 1995, *15th Int. Display Res. Conf.* (SID, Hamamatsu), p. 707.
[5] Kondo, K., Konishi, N., Kinugawa, K., and Kawakami, H., 1995, *Proc. 2nd Int. Display Workshop* (SID, Hamamatsu), p. 43.
[6] Oh-e, M., and Kondo, K., 1995, *Appl. Phys. Lett.*, **67,** 3895.
[7] Oh-e, M., Yonaya, M., Ohta, M., and Kondo, K., 1997, *Liq. Cryst.*, **22,** 391.
[8] Born, M., and Wolf, E., 1980, *Principles of Optics* (Pergamon, New York).
[9] De Gennes, P. G., 1974, *The Physics of Liquid Crystals* (Oxford University Press, Oxford).
[10] Chandrasekhar, S., 1977, *Liquid Crystals* (Cambridge University Press, Cambridge).
[11] Leslie, F. M., 1970, *Mol. Cryst. liq. Cryst.*, **12,** 57.
[12] Oh-e, M., and Kondo, K., 1997, *Jpn. J. appl. Phys.*, **36,** 6798.
[13] Oh-e, M., Yonaya, M., and Kondo, K., 1997, *J. Appl. Phys.*, **82,** 528.
[14] Oh-e, M., and Kondo, K., 1996, *Appl. Phys. Lett.*, **69,** 623.
[15] Oh-e, M., Umeda, Y., Ohta, M., Aratani, S., and Kondo, K., 1997, *Jpn. J. Appl. Phys.*, **36,** L1025.